Hindawi
Advances in Materials Science and Engineering
Volume 2021, Article ID 8816593, 14 pages
https://doi.org/10.1155/2021/8816593

Research Article

A Kind of Filling Lattice Structure Based on DFAM for Mechanical Parts: The Diamond Lattice Structure

Xuan Yin,[1] Wenjun Meng,[1] Jinzhao Cheng,[2] Hailong Wang,[3] and Xiaoxia Zhao[1]

[1]*School of Mechanical Engineering, Taiyuan University of Science and Technology, Key Laboratory of Intelligent Logistics Equipment in Shanxi Province, Taiyuan, Shanxi 030024, China*
[2]*Shanxi Traffic Vocational and Technical College, Taiyuan, Shanxi 030031, China*
[3]*China National Heavy Machinery Corporation, Haidian, Beijing 100036, China*

Correspondence should be addressed to Wenjun Meng; tyustmwj@126.com

Received 15 September 2020; Revised 18 December 2020; Accepted 31 December 2020; Published 16 January 2021

Academic Editor: Carlo Santulli

Thanks to the geometric and material complexity of additive manufacturing, the design space of mechanical parts has been developed, in which lattice filling structure customization can be applied to the solid filling of mechanical parts to achieve the goal of mechanical structure lightweight. A kind of diamond lattice structure unit is designed by imitating the natural method based on Design for Additive Manufacturing of mechanical parts. The mathematical model of the relative density and mechanical properties of the unit are established, and the relationship between the two is obtained, which is verified by simulations; then the relatively uniform results are obtained. The variable density hypothesis of diamond lattice structure is proposed, the methods of simulations and compression tests are used to verify the hypothesis, and the results show that the variable density structure with the density of the filling element decreasing gradually with the stress point as the center has better compression performance and concurrently verify the correctness and applicability of the equivalent modulus of elasticity mathematical model. The results of this study can be applied to the solid sandwich filling of pressure mechanical parts, and the stress density matching relationship can be carried out to further specific design.

1. Introduction

The characteristics of additive manufacturing, such as geometric complexity and material complexity, provide new opportunities for customization of products, which also develop new design space for designers. The concept of Design for Additive Manufacturing (DFAM) emerged.

Design for Additive Manufacturing (DFAM) is defined as follows [1, 2]: The process of achieving expected performance and other life cycle objectives within the capability of additive manufacturing through the synthesis of shape, size, hierarchy, and material composition. DFAM, which gives full play to the customizable and multifunctional characteristics of additive manufacturing, focuses on maximizing the functional value of products. The design freedom of additive manufacturing [3] is shown in Figure 1.

Different from the reduction process, additive manufacturing allows complex structural adjustment from the inside without additional manufacturing costs. Therefore, the application of sandwich structure as an important embodiment of additive manufacturing structure design is conducive to the lightweight of parts. Lattice structure is a kind of structure which is easy to be parameterized and controlled. Taking it as the basic unit of sandwich structure is the basis of this paper.

Lattice structure is a kind of periodically connected space filling element, which is usually created by truss structure and minimalist surface [4], which not only has the advantages of saving materials, reducing energy use, and saving time, but also has high energy absorption rate, high-strength weight ratio, and thermal management ability. The lattice structure has not been widely used in the past due to the limitation of processing methods, and the rise of additive

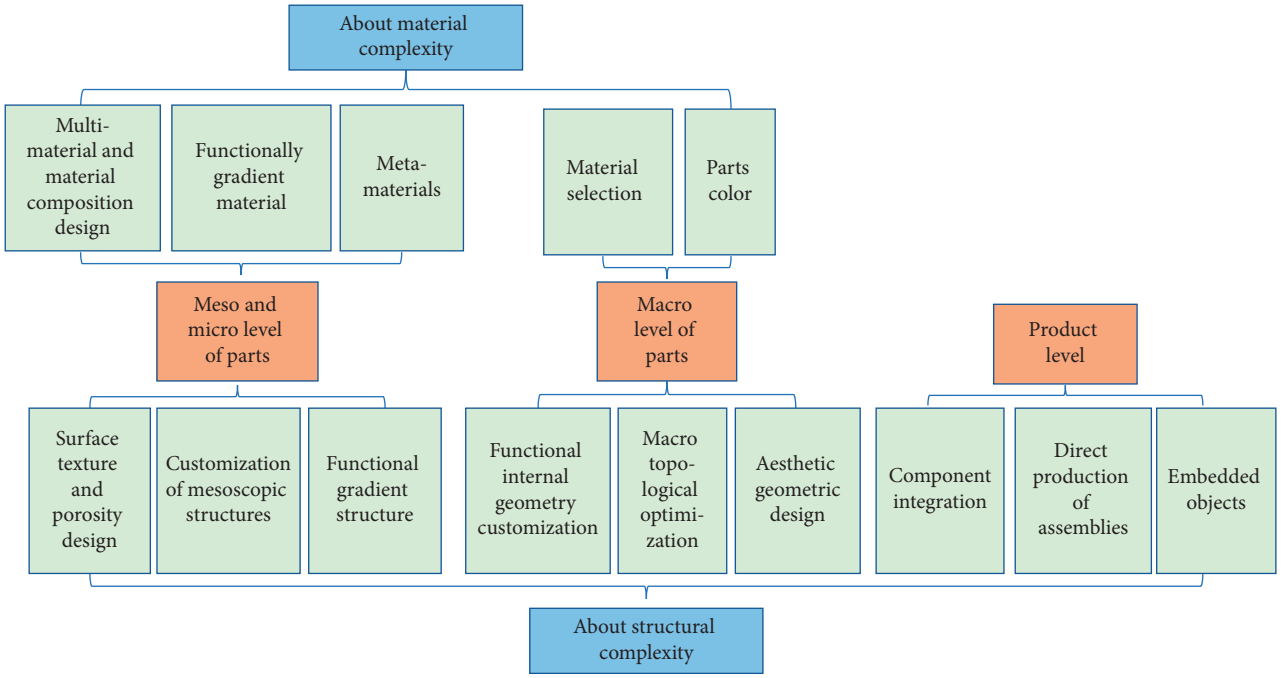

Figure 1: Design freedom of additive manufacturing.

manufacturing makes mesoscopic lattice structure get a lot of attention and research.

Rosen [2] and others [1, 5] of Georgia Institute of Technology in the United States have carried out systematic research on DFAM and proposed systematic design method of cellular structure. Li Yang and others of the University of Louisville in the United States have carried out theoretical and experimental research on metal cellular unit made of AM and summarized the size effect of cellular structure [6, 7]. Sustainable Manufacturing and Life Cycle Engineering Research Group of the University of New South Wales in Australia is also committed to the research of lattice structure; the design, analysis and manufacture of lattice structure are reviewed [4]; in addition, it cooperates with Supachai Vongbunyong in Thailand to develop the integrated software tool for cellular structure design [8]. The research team of Universidade de Lisboa in Portugal has done in-depth research on the mechanical properties of the lattice structure [9, 10]. Ahmed Yussuf Hussein of the University of Exeter in UK has studied the development of light porous structure of metal additive manufacturing [11]; in addition, many scholars have done a lot of research on the additive manufacturing and mechanical properties of porous metal biomaterials [12, 13]. Panda of the National Institute of Technology in India designed and developed the cellular structure of additive manufacturing [14]. In China, Beijing University of Science and Technology is dedicated to the research of spatial porous structure; Song et al. proposed an effective optimization method for the design of irregular cellular structure [15]. Zhao et al. studied the design method of variable-density porous structure based on local relative density mapping [16]. Liu et al. from Beijing University of Aeronautics and Astronautics studied the design method of honeycomb structure generation for additive manufacturing [17]. Liao et al. of South China University of Technology proposed a topological optimization-based variable density lattice structure optimization design method [18].

It is not difficult to find that the research on the lattice structure of additive manufacturing is relatively limited at this stage. Most of the lattice structure units are conventional which are generated manually; few of them are optimized design. Most of the lattice structures are in periodic arrangement, lacking the variable scale mapping of the functional requirements. In addition, the experimental research on the lattice structure is very rare, so the simulation analysis cannot be verified, and the parameter optimization of the lattice structure has no experience to follow.

This paper focuses on the theoretical and experimental study of the lattice structure with variable density based on compressive stress. In this paper, a kind of optimized lattice structure unit is proposed. A fine mathematical model of lattice structure density and elastic modulus is established on the premise of considering deformation cross section. On this basis, a series of simulation and experiment methods are used to verify the correctness of the above theory.

2. Lattice Structure Unit Design

The spatial lattice structure mentioned in the existing literature includes octahedral structure, body centered cubic structure, and orthotropic cubic structure. There are many rods connected at the joints of these structures, which is easy to cause stress concentration and rod waste. Furthermore, in the context of additive manufacturing, the lattice structure unit should not be limited to the traditional regular

structure, but should be combined with the load-bearing situation of parts to find the most suitable internal lattice structure unit under specific load.

There are some natural structures in nature, which have unique advantages under some stress conditions. For example, the spider web structure has great tension, the laminated structure of plant stem makes its bending and torsion resistance remarkable, the vein structure of lotus leaf makes its pressure bearing capacity extremely strong, and the honeycomb structure has a certain strength while playing its accommodation function.

Diamond is one of the substances with the highest hardness in the world; because each C atom in its crystal is connected with four C atoms around it by covalent bond with the same angle, the inter atomic force is quite firm, which makes the material very stable. This kind of natural and superior molecular structure is worth learning from in the design of lattice structure. In this paper, a preliminary study on the lattice elements of pressure parts is carried out by using the simulated natural design.

2.1. Three-Dimensional Modeling of Diamond Lattice Structure. The diamond lattice structure unit (DLSU) designed in this paper is shown in Figure 2. C atom is replaced by node and covalent bond is replaced by rod. Each node and four surrounding nodes are connected by rods to form space tetrahedron structure. The lengths of rods are equal, and the angle between rods is $109^\circ\,28'(109.47^\circ)$. Fillet transition connection is designed between nodes and rods in order to increase the stability of slender members. This kind of structure with space center symmetry has relatively uniform internal force, and only four rods are connected to each node, resulting in a smaller stress concentration at the node, which is more robust than the ordinary structure.

In order to divide the solid into space grids in the design and parametric modeling of the later structure, the concept of structural cell is introduced. The space of each structural unit is Hexagonal Prism (HP) cell, as shown in Figure 3; the structural cells are connected end to end to fill the solid structure without gaps.where $\varnothing$ is the diameter of the inner tangent circle of the hexagonal prism; h is the height of HP cell; b is the bottom edge length of HP cell; and l is the rod length of the DLSU. After calculation, the parameter relationships are as follows:

$$h = \frac{\sqrt{6}}{3}\varnothing,$$
$$l = \frac{\sqrt{6}}{4}\varnothing, \tag{1}$$
$$b = \frac{\sqrt{3}}{3}\varnothing,$$

2.2. Calculation of Cell's Relative Density of Diamond Lattice Structure. According to the Gibson–Ashby micromechanical model of porous structure (1997), the equivalent mechanical properties of lattice structure, such as elastic modulus, shear modulus, yield strength, etc., are all represented by polynomials related to the relative density of lattice structure. The relative density of lattice structure can be expressed as

$$\rho_x = \frac{V_s}{V_c}, \tag{2}$$

where ρ_x represents the relative density of structural cell; V_s is the volume of solid part in structural cell; and V_c is the total volume of structural cell, for HP cell $V_c = (\sqrt{2}/2)\varnothing^3$.

2.2.1. The Case of Low Density. The rods constituting the unit structure are slender rods with poor stability when the relative density is low. Therefore, the lattice unit structure with spherical nodes and fillet transition is adopted. The schematic diagram is shown in Figure 4, in which the volume of equivalent rod is accurately calculated by equation (3).

$$V_g = \pi r^2 \cdot \left[l - 2\sqrt{(R-r)\left(R+r+2R_y\right)}\right] + 2\pi\left[\int_0^m g^2(y) - \int_{\sqrt{(R-r)\left(R+r+2R_y\right)}-R}^{m} f^2(y)\,\mathrm{d}y\right]. \tag{3}$$

In the design, the rod is the main force object, and its volume and mechanical properties are changed by changing its section radius r. The node, as the auxiliary structure of stress, the determination of its size mainly follows the principle of noninterference of intersecting line. Therefore, the node radius R should be determined by the rod radius r and the fillet radius R_y; that is, $R = (\sqrt{6}/2)r + ((\sqrt{6}-2)/2)R_y$.

The calculation process of relative density of structure cell is shown in Table 1. The fillet radius $R_y = r$ is selected to simplify the calculation; the final results are as follows:

$$\rho_x = 10.8833\left(\frac{r}{\varnothing}\right)^2 - 20.1912\left(\frac{r}{\varnothing}\right)^3. \tag{4}$$

It can be seen that the value of relative density is a cubic function of the ratio of the section radius of the rod r to the cell parameter $\varnothing$. When the ratio increases gradually, the space interference of the nodes geometric structure will be formed, which should be avoided by controlling the ratio in the range of $0 \le r/\varnothing \le \sqrt{3}/8$.

2.2.2. The Case of High Density. The spherical node is changed into an ordinary node as the stability increases with the increasing relative density of the unit; that is, the rods are directly connected. The structure unit and the analyzed equivalent rods are shown in Figure 5, in which (a) shows the basic unit of diamond lattice structure after omitting the spherical node and fillet; (b), (c), and (d) show the equivalent rod and its partial enlarged drawing after unit superposition. It can be seen from Figure 5(d) that the two ends of the equivalent rods are all three equal sector sections with variable radius. As shown in Figure 5(e), the equivalent rod is made up into a cylindrical rod in order to calculate the volume. 5(f) is shown to establish a Cartesian coordinate

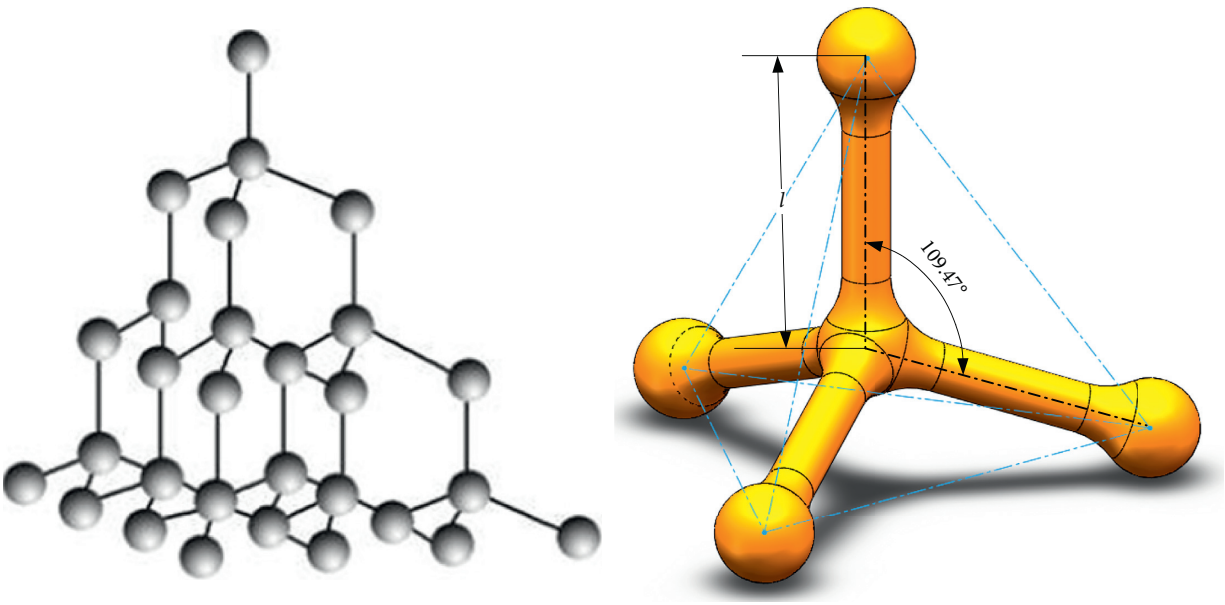

Figure 2: The diamond lattice structure unit.

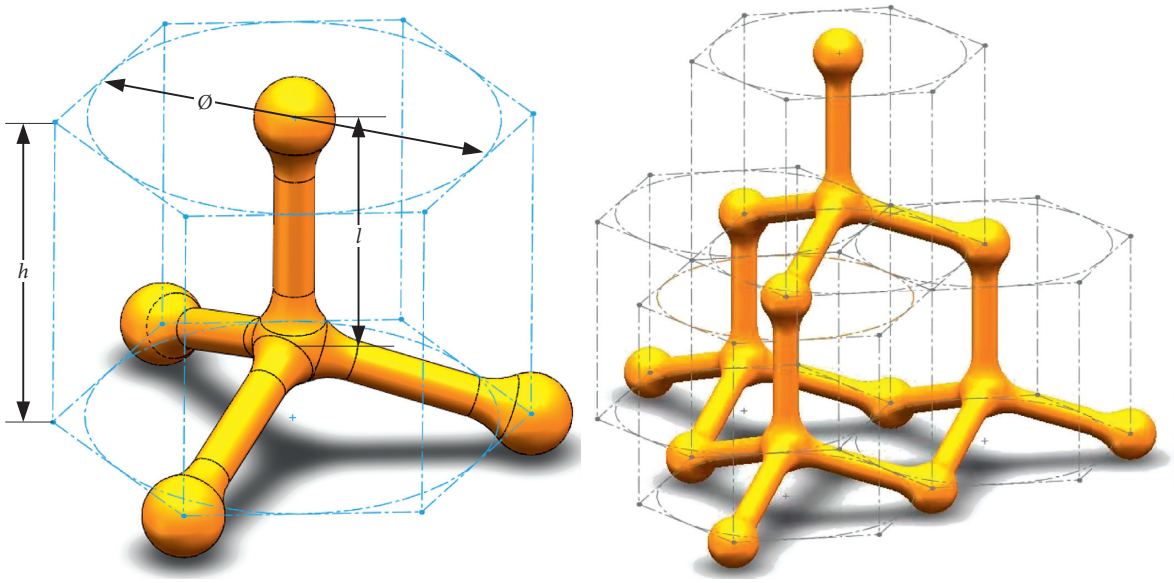

Figure 3: HP cell and its superposition.

system for the complete cylindrical rod, by which calculating the volume of the equivalent rod shown in Figure 5(c), and thus establishes a mathematical model for the relative density of lattice DLSU with ordinary nodes.

In Figure 5(f), the sector plane A is expressed as $z = x/\tan(109.47^\circ/2)$, the Cartesian coordinate system is transformed into polar coordinate system for the convenience of calculation, where $x = \rho \cos \theta$, $y = \rho \sin \theta$, and $\mathrm{d}x\mathrm{d}y = \rho\mathrm{d}\rho\mathrm{d}\theta$, and the complement part is divided, calculated, and then removed to obtain the volume of the equivalent rod:

$$V_{g'} = \pi r^2 l - 12 \int_0^{\pi/3} \int_0^r \frac{\rho \cos \theta}{\tan(109.47^\circ/2)} \rho \mathrm{d}\rho \mathrm{d}\theta, \tag{5}$$

where r is the section radius of the rod, l is the length of the rod (related to the cell size), and the integral region D is the sector region with radius r and included angle of 120°.

The relative density of HP cell is $\rho_x = 4\sqrt{2}V_{g'}/\varnothing^3$. The calculation result is as follows:

$$\rho_x = 2\sqrt{3}\pi\left(\frac{r}{\varnothing}\right)^2 - 8\sqrt{6}\left(\tan\frac{109.47^\circ}{2}\right)^{-1}\left(\frac{r}{\varnothing}\right)^3. \tag{6}$$

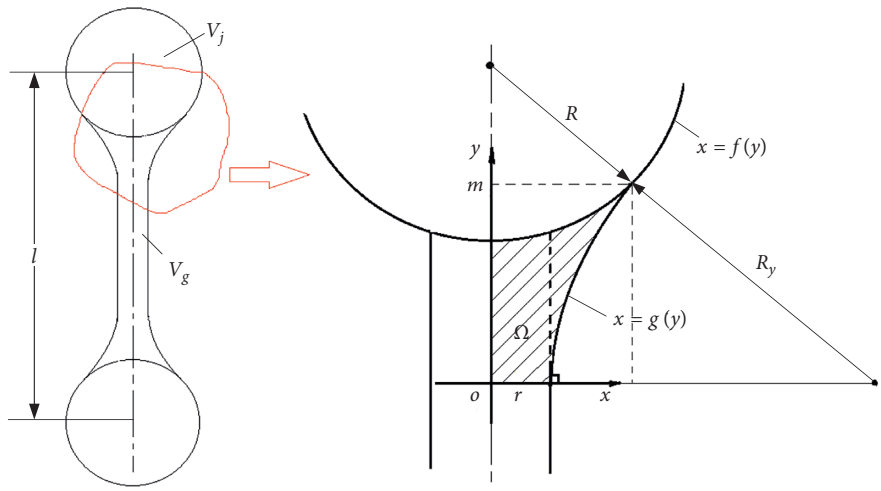

Figure 4: Model of fillet connection between node and rod.

Table 1: Calculation process of relative density.

Parameters	HP cell
Mesh parameter	Inscribed circle diameter $\varnothing$
Solid volume parameters	Rod section radius r, joint fillet radius R_y, mesh parameter $\varnothing$
Number of equivalent nodes (n_j)	2
Number of equivalent rods (n_g)	4
Length of equivalent rod (l)	$(\sqrt{6}/4)\varnothing$
Length of rod transition area (m)	$R_y\sqrt{(\sqrt{6}-2)r((\sqrt{6}r+2)R_y)}/(\sqrt{6}-1)r+R_y$
Volume of equivalent node (V_j)	$\frac{4}{3}\pi(\frac{\sqrt{6}}{2}r+\frac{\sqrt{6}-2}{2}R_y)^3$
Volume of equivalent rod (V_g)	$\pi r^2\cdot[l-2\sqrt{(R-r)(R+3r)}]+2\pi[\int_0^m g^2(y)\mathrm{d}y-\int_{\sqrt{(R-r)(R+3r)}-R}^m f^2(y)\mathrm{d}y]$
Solid volume (V_s)	$V_s=n_jV_j+n_gV_g$
Structure cell volume (V_c)	$(\sqrt{2}/2)\varnothing^3$
Relative density ($\rho_{\mathbf{x}}$)	$\sqrt{2}(n_jV_j+n_gV_g)/\varnothing^3$

From the properties of the function in formulae (5) and (8), it can be seen that the ratio of the section radius r of the element member to the cell size parameter (a or $\varnothing$) is an important value, which is recorded in this paper as parameter ratio. The larger the parameter ratio is, the closer the structure is to the solid. When the relative density ρ_x equals 1, the structure appears as a solid in the macroscopic aspect, while the parameter ratio should be within the range of $r/\varnothing \le 0.5239$, which makes the relative density ρ_x meaningful.

2.2.3. Cell's Relative Density of Diamond Lattice Structure. The conclusions in sections 2.2.1 and 2.2.2 are combined to form the mathematical models of the relative density of the HP cell of the diamond lattice structure, as shown in the following equation:

$$\rho_x = \begin{cases} 10.8833\left(\frac{r}{\varnothing}\right)^2 - 20.1912\left(\frac{r}{\varnothing}\right)^3, & 0 < \frac{r}{\varnothing} \le \frac{\sqrt{3}}{8}, \\ 2\sqrt{3}\pi\left(\frac{r}{\varnothing}\right)^2 - 8\sqrt{6}\left(\tan\frac{109.47^\circ}{2}\right)^{-1}\left(\frac{r}{\varnothing}\right)^3, & \frac{\sqrt{3}}{8} < \frac{r}{\varnothing} \le 0.5239. \end{cases} \tag{7}$$

The function value ρ_x obtained by different parameter combinations of the combined mathematical model varies from 0 to 1. Plot the function to get the result shown in Figure 6.

The contour lines of function value shown in horizontal plane 0 in Figure 6 are a series of straight lines passing through the origin, which indicates that when the parameter ratio $r/\varnothing$ is fixed, the relative density is the same, and with the increase of parameter ratio, the relative density increases nonlinearly.

3. Equivalent Mechanical Properties of Diamond Lattice Structure

3.1. Equivalent Elastic Modulus of Diamond Lattice Structure. As shown in Figure 7(a), stress σ is applied on the cell of diamond lattice structure, which results in deformation of lattice structure. The dotted line in Figure 7(b) represents the original structural axis, and the solid line represents the deformed structural axis. Since rods are rigidly connected with each other, the included angle between the tangent lines of each rod end at the rigid node O remains unchanged after deformation. In order to obtain the equivalent elastic modulus, the displacement at point A is required, that is, the total deformation of the unit Δl.

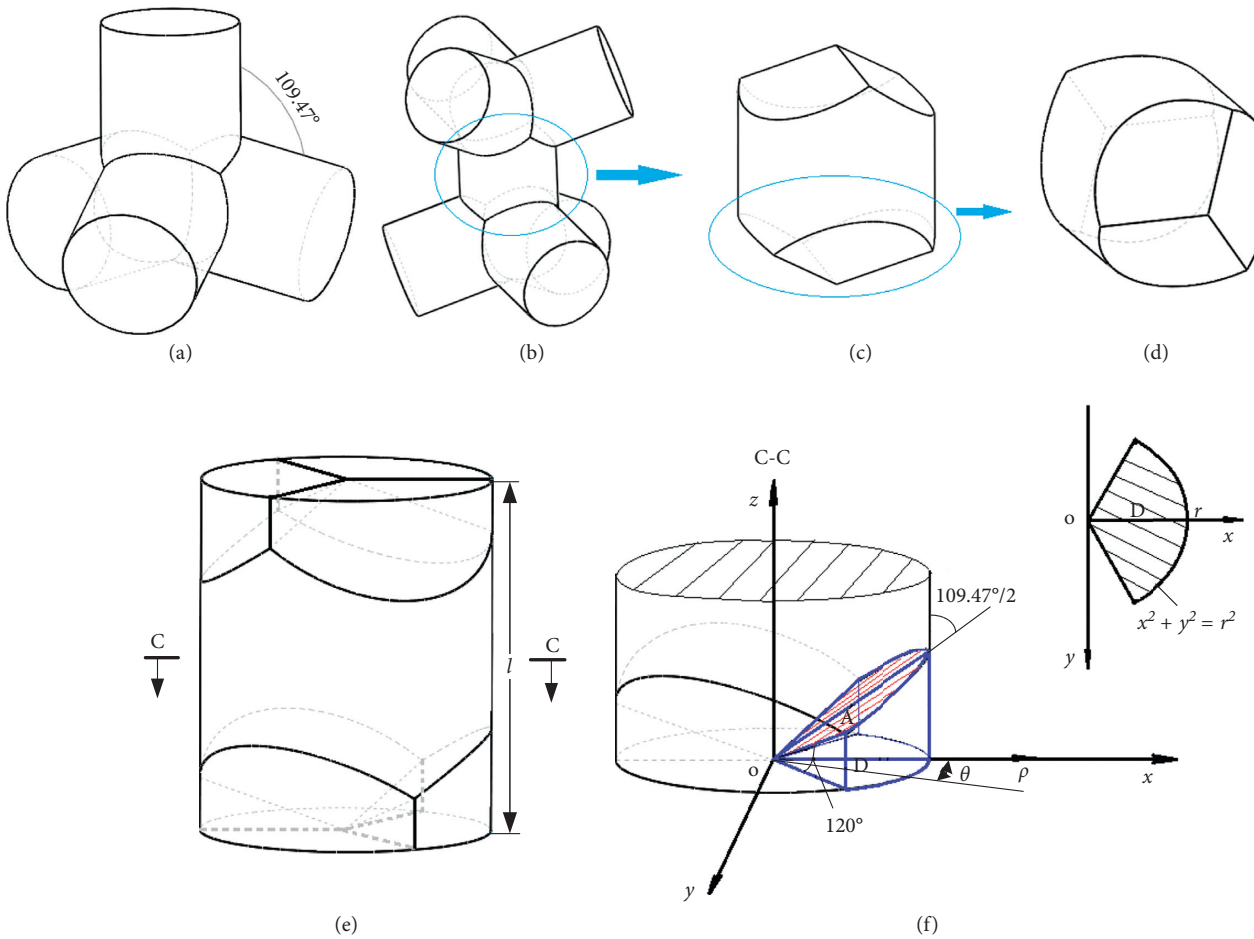

Figure 5: DLSU with ordinary nodes and their equivalent rods.

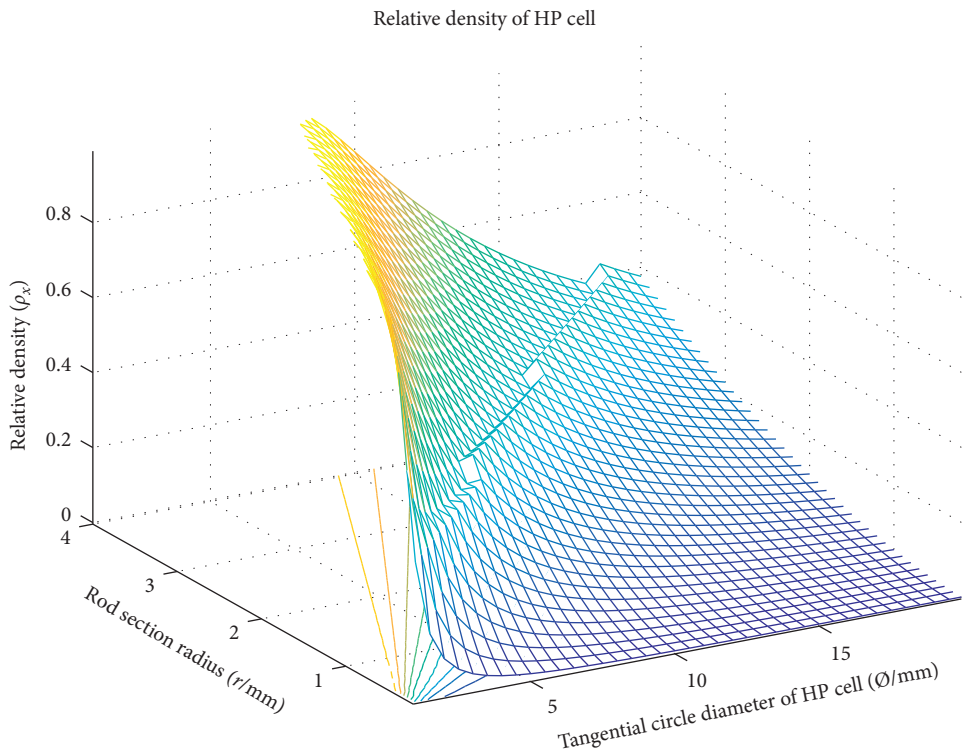

Figure 6: Final results of structure cell relative density.

According to the functional principle, the work done by the pressure is equal to the stored energy of rods [19]; that is, the work done by the external force is equal to the sum of the strain energy of the rod system in numerical value, which is expressed as follows:

$$\frac{1}{2}F\Delta l = U_1 + U_2, \tag{8}$$

where U_1 is the sum of strain energy in tension and compression and U_2 is the sum of strain energy in bending. It shows that the total deformation of the structure unit can be obtained by calculating the strain energy of each rod. The specific analysis is as follows.

Figure 8(a) is the force analysis of the rod. There is no slip in the horizontal direction on node O for its resultant force in the horizontal direction is 0, so that node O displaces only in the vertical direction. In order to learn the strain energy conveniently, the node O is set as the fixed point, and the rods OA and OB are taken as the research objects for the force and deformation analysis.

The resultant force of OA rod is an axial force of F, which leads to tension and compression deformation. For OB rod, the force F_B is decomposed into axial force and vertical force to obtain the forces N and P, respectively, and the rod is subject to axial force and bending moment M, resulting in tension and compression deformation and bending deformation. According to the symmetry of the structure and the uniformity of the force, the force condition of rods OC and OD is the same as that of OB. Therefore, tension and compression strain energy is produced in all the rods of the deformed unit, and bending strain energy is produced in the rods OB, OC, and OD.

The equations of strain energy in tension and compression and in bending are, respectively, as follows:

$$U_1 = \int_0^l \frac{F^2(x)}{2\mathrm{EA}(x)}\mathrm{d}x, \tag{9}$$

$$U_2 = \int_0^l \frac{M^2(x)}{2\mathrm{EI}}\mathrm{d}x, \tag{10}$$

where E represents the inherent elastic modulus of the raw material.

$F(x)$ in equation (9) is a function of the force on the rod, which is a constant function in this example. $A(x)$ is a function of the cross-sectional area of the rod. Due to the complexity of the change of the cross-sectional dimension of the designed member, as shown in Figure 8(b), the profile of the rod is simplified from the change of curved surface to the change of wedge shape for the convenience of calculation. In this research,

$$A(x) = \begin{cases} \pi[(\sqrt{6}-1)r - (\sqrt{3}-\sqrt{2})x]^2, & 0 \le x \le \sqrt{2}\,r, \\ \pi r^2, & \sqrt{2}\,r < x < l - \sqrt{2}\,r, \\ \pi[(\sqrt{6}-1)r - (\sqrt{3}-\sqrt{2})(l-x)]^2, & l - \sqrt{2}\,r \le x \le l. \end{cases} \tag{11}$$

In equation (10), $M(x)$ is a function of bending moment, which of OB rod is

$$M(x) = P\left(x - \frac{l}{2}\right). \tag{12}$$

The value of P is $F_B\cos 19.47^\circ$. I is the section moment of inertia of the rod, that of cylinder section is $I_0 = \pi r^4/4$; for the wedge section, the reduced moment of inertia of the variable section rod I_z is calculated as follows [20]:

$$I_z = \frac{16}{(1/I_1) + (2/I_2) + (9/I_3) + (4/I_4)} = \frac{\pi r^4}{1.3159}, \tag{13}$$

where I_1, I_2, I_3, and I_4 are the section moments of inertia when $x = (3\sqrt{2}/4)r$, $x = (\sqrt{2}/2)r$, $x = (\sqrt{2}/4)r$, and $x = 0$, respectively, as shown in Figure 8(b).

In conclusion, the total tensile and compressive strain energy of the structure unit is as follows:

$$U_1 = U_{1OA} + 3U_{1OB} = \int_0^l \frac{F^2}{2EA(x)}\mathrm{d}x + 3\int_0^l \frac{N^2}{2\mathrm{EA}(x)}\mathrm{d}x. \tag{14}$$

The value of N is $F_B\sin 19.47^\circ$. The total bending strain energy of the rods in the structure unit is expressed as follows:

$$\begin{aligned} U_2 &= 3U_{2OB} = 3\int_0^l \frac{M^2(x)}{2\mathrm{EI}}\mathrm{d}x \\ &= 3\left[\int_0^{\sqrt{2}\,r} \frac{M^2(x)}{2\mathrm{EI}_z}\mathrm{d}x + \int_{\sqrt{2}\,r}^{l-\sqrt{2}\,r} \frac{M^2(x)}{2\mathrm{EI}_0}\mathrm{d}x + \int_{l-\sqrt{2}\,r}^{l} \frac{M^2(x)}{2\mathrm{EI}_z}\mathrm{d}x\right]. \end{aligned} \tag{15}$$

From the above calculation process, it can be observed that rod OA mainly bears load by tension and compression deformation, while rods OB, OC, and OD have very small tension and compression deformation and mainly bear load by bending deformation.

From the above equations (8) ~ (15), the total deformation of the structure can be obtained. That is,

$$\Delta l = \frac{\sigma}{\pi E}\left(0.0196\frac{\varnothing^5}{r^4} - 0.1826\frac{\varnothing^4}{r^3} + 2.0220\frac{\varnothing^3}{r^2} - 2.1427\frac{\varnothing^2}{r}\right). \tag{16}$$

Therefore, the equivalent elastic modulus E^* of diamond lattice structure is obtained by equation (17)

$$E^* = \frac{\sigma}{\varepsilon} = \frac{\sigma\Delta h}{\Delta l}, \tag{17}$$

where ε represents the strain produced by the stress of the structure cell and h is the original height of the cell, whose value is $\sqrt{6}/3\varnothing$. After sorting out, the following result is obtained:

$$E^* = \frac{E}{0.0077(\varnothing/r)^4 - 0.0712(\varnothing/r)^3 + 0.7883(\varnothing/r)^2 - 0.8353(\varnothing/r)}. \tag{18}$$

Obviously, the equivalent elastic modulus of diamond lattice structure is related to the elastic modulus E of the raw material itself and the parameter ratio of structure

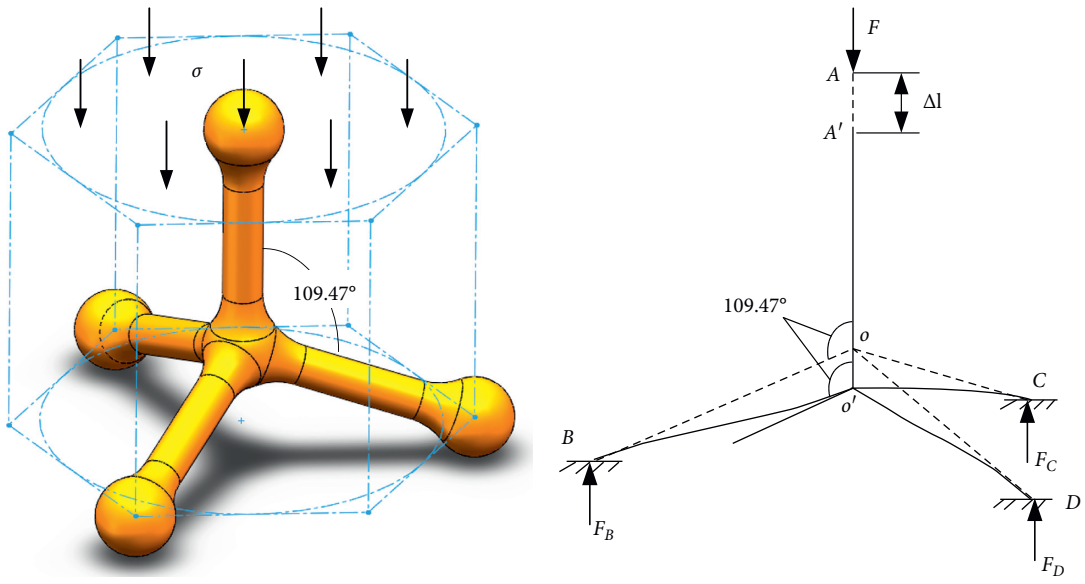

Figure 7: Stress and deformation diagram of structure cell.

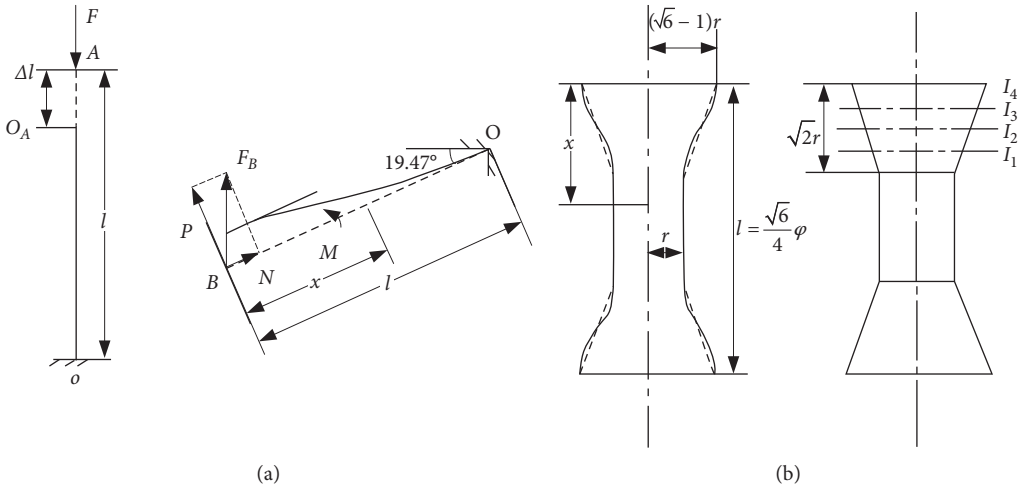

Figure 8: Force analysis and profile simplification of rods.

cell $\varnothing/r$; the parameter ratio here is the inverse of that described in Section 2. The value of E/E^* is a quartic function of the parameter ratio $\varnothing/r$, while from the above study, it is concluded that the relative density is a cubic function of the parameter ratio $\varnothing/r$; it is shown that the equivalent elastic modulus E^* has a nonlinear relationship with the relative density ρ_x. Therefore, when the parameter ratio is fixed, the relative density and the equivalent elastic modulus of diamond lattice structure are fixed, respectively. After calculation, the following relationship is obtained:

$$E^* = E\left(0.4239\rho_x^{3/2} - 0.0008\right). \tag{19}$$

3.2. Simulation of Mechanical Properties of Diamond Lattice Structure Unit. For lattice structure, the stress-strain curve changes with the increase of relative density, and the corresponding elastic modulus, plastic yield stress, and ultimate stress of brittle fracture increase [21]. With the increase of the parameter ratio $r/\varnothing$, the density of diamond structure increases, and the mechanical properties change.

A structure unit is intercepted to simulate the upper unit transferring three equal forces F along the direction of the rods, and the stress state of the unit under different relative density is observed. When the maximum stress of the structure reaches the yield stress, the value of F reaches the upper limit, which is recorded as $F_{\max}$. Aluminum alloy 1061 was selected as the simulation material, with yield stress of

27.57 MPa and elastic modulus of 69 GPa. Figure 9 shows the mechanical simulation analysis of diamond lattice structure units under different rod section radius (0.5 mm, 1.0 mm, 1.5 mm, and 2 mm) when the inner tangent diameter of HP cell section ∅ is 10 mm. It can be seen from the von Mises stress that the most dangerous point of the structure occurs at the joint between the node and the rod.

As seen in Table 2 which shows the comparison of simulation result data, the larger the section radius r of the rod, the greater the relative density of the structure, the greater the load-bearing capacity, and the smaller the deformation of the structure; all these changes are nonlinear as shown in Figure 10.

Comparing the equivalent elastic modulus E_1^* calculated by the simulation data with the equivalent elastic modulus E_2^* calculated by the above theoretical research, as shown in Figure 11, the overall trend of the curve is consistent.

However, with the increase of the parameter ratio, the bending moment condition of OB, OC, and OD rods in the model changes into the shear condition. Therefore, the actual equivalent elastic modulus of the lattice structure is higher than the calculated value of the theoretical model in the region of high parameter ratio, as shown in Figure 11. The existence of this gap makes it necessary to adjust the theoretical model for the high parameter ratio in future work.

4. Variable Density Design of Diamond Lattice Structure

4.1. Variable Density Hypothesis and Simulation Verification. When the structure is stressed, the internal stress decreases with the increase of the distance from the stressed point. According to the above research, the load-bearing capacity of the structure increases with the increase of the relative density of the structure.

In the observation of organisms in nature, their tissues are often distributed in areas with large stress and deformation, in order to keep the original shape and physiological function of organism under external load without damage. Some organisms can dynamically adjust the flow direction of internal tissue to the area according to the specific position of external load, so as to reduce the influence of stress and deformation on themselves.

Therefore, according to the tissue distribution law of natural organisms and the above research conclusions, it is assumed that the variable density structure has better bearing capacity; that is, with the distance from the stress point, the structure density is smaller and smaller, and such structure combination is better than the equal density structure.

According to the hypothesis, the diamond structure is designed with variable density by changing the section radius distribution of the rods filled with lattice cell on the premise that the total material volume and total relative density of the structure remain unchanged. The constant density structure cell is adjusted by variable density, and the stress distribution and displacement are simulated and compared under the same stress conditions; the calculation results shown in Figures 12 and 13 are obtained, respectively.

From Figure 12, it can be seen intuitively that for the equal volume structure of materials under the same stress condition, the superposition of internal variable density units makes the structure stress distribution more uniform than that of constant density units. The maximum stress is also reduced from 23.65 MPa to 18.34 MPa, a decrease of 22.45%. As seen from Figure 13, the maximum displacement, which occurs in the stress center of the structure, is reduced from 3.320×10^{-3} to 2.587×10^{-3} mm, a decrease of 22.08%. It shows that the structure adjusted by variable density according to stress conditions can bear more force and the stress distribution of the whole structure is more uniform and reasonable. The above hypothesis is verified.

4.2. Additive Manufacturing and Compression Contrast Test of Diamond Lattice Structure. AlSi10 Mg aluminum alloy powder is used to make diamond lattice structure by SLS technology. The mechanical properties of the material are as follows: modulus of elasticity 70 ± 5 GPa, yield strength 245 ± 10 MPa, and forming accuracy of 0.05 mm; the formed structure is shown in Figure 14. From left to right, there are traditional octahedral lattice structure, constant density diamond lattice structure, and variable density diamond lattice structure, and they are named specimen 1, specimen 2, and specimen 3, respectively. Various variables of the three kinds of specimens, including total volume, size, relative density of lattice part, and thickness of upper and lower bottom surfaces, are designed to be equal. A stress boss with a thickness of 2 mm is designed at the center of the top of the structure to simulate the local stress of the structure.

The compression tests are carried out on the universal mechanical testing machine, and the force-displacement curves shown in Figure 15 are finally obtained.

The test curves are analyzed as follows:

First of all, the three kinds of specimens have gone through the elastic stage, yield stage, and strengthening stage in the compression process. Their curves basically coincide in the elastic stage and yield stage because they are of the same relative density, and they all enter into a short yield stage when the pressure is about 13 kN. Secondly, the three kinds of specimens show different trends in the strengthening stage: the displacement of specimen 1 changes faster and faster with the increase of force until the bottom edge of the specimen breaks; specimen 2 and specimen 3 show higher compressive capacity in the strengthening stage, and the displacement basically increases at a constant speed with the increase of force, but small cracks appear due to the problem of the forming quality of the specimen, resulting in the trend of the force-displacement curve being step like in the later stage until reaching the failure condition. Specimens 2 and 3 do not form obvious fracture on the structure after failure.

Finally, the failure loads of the three kinds of specimens are 21.1 kN, 28.1 kN, and 38.8 kN, respectively. It can be seen through comparison that the compressive strength of specimen 3 is higher than that of specimen 2.

Table 3 is the analysis and comparison of the compression test results. The average equivalent modulus of elasticity of the diamond lattice structure specimens

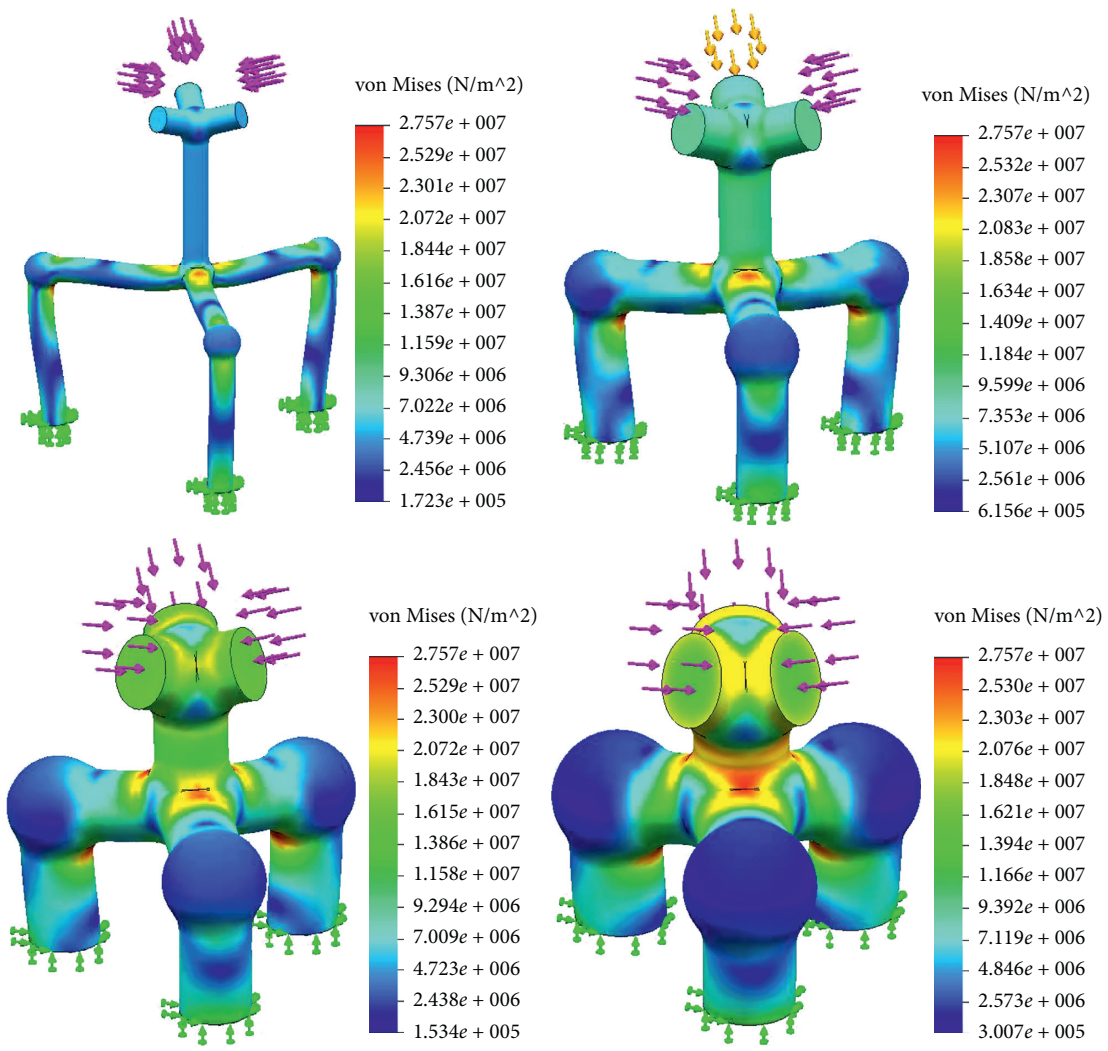

Figure 9: Simulation analysis of diamond lattice structure unit.

Table 2: Comparison of simulation data of diamond lattice structure unit.

Serial number	Rod section radius r (mm)	Relative density ρ_x	Force F_{max} (N)	Maximum stress σ_s(MPa)	Maximum displacement s (mm) ($\times 10^{-3}$)	Simulation equivalent modulus of elasticity E_1^* (GPa)	Theoretical equivalent modulus of elasticity E_2^* (GPa)
1	0.5	0.0265	3.644	27.57	5.602	0.0617	0.0710
2	0.6	0.0375	6.573	27.57	4.913	0.1261	0.1572
3	0.7	0.0507	10.700	27.57	4.407	0.2289	0.2787
4	0.8	0.0657	15.902	27.57	3.971	0.3776	0.4374
5	0.9	0.0825	24.319	27.57	3.811	0.6016	0.6379
6	1.0	0.1011	32.346	27.57	3.610	0.8448	0.8850
7	1.1	0.1214	42.697	27.57	3.440	1.1702	1.1820
8	1.2	0.1433	56.201	27.57	3.371	1.5718	1.5315
9	1.3	0.1669	70.797	27.57	3.264	2.0450	1.9391
10	1.4	0.1921	88.592	27.57	3.218	2.5956	2.4075
11	1.5	0.2188	110.539	27.57	3.231	3.2256	2.9383
12	1.6	0.2469	130.450	27.57	3.112	3.9521	3.5331
13	1.7	0.2765	160.650	27.57	3.173	4.7735	4.1974
14	1.8	0.3075	190.280	27.57	3.147	5.7006	4.9323
15	1.9	0.3398	219.681	27.57	3.063	6.7619	5.7384
16	2	0.3734	250.636	27.57	2.966	7.9671	6.6186

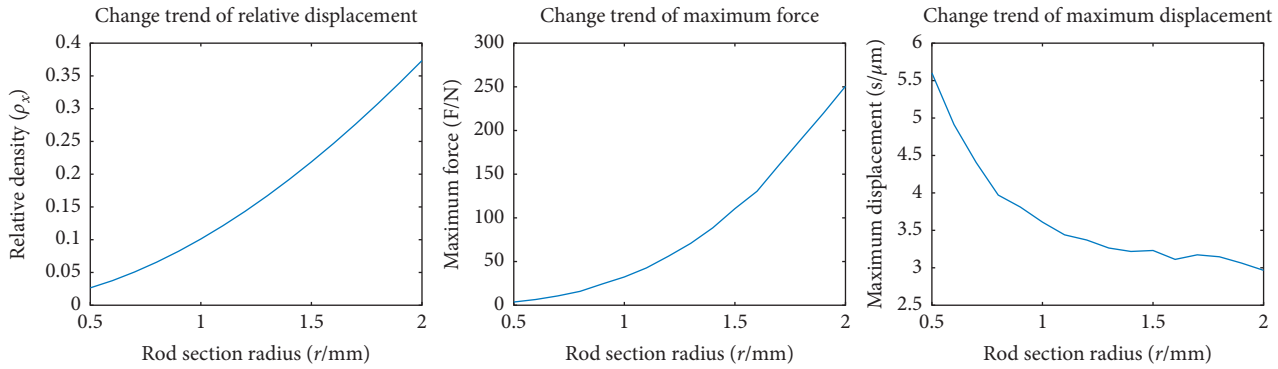

Figure 10: Variation trend of parameters of structure unit with section radius of rod.

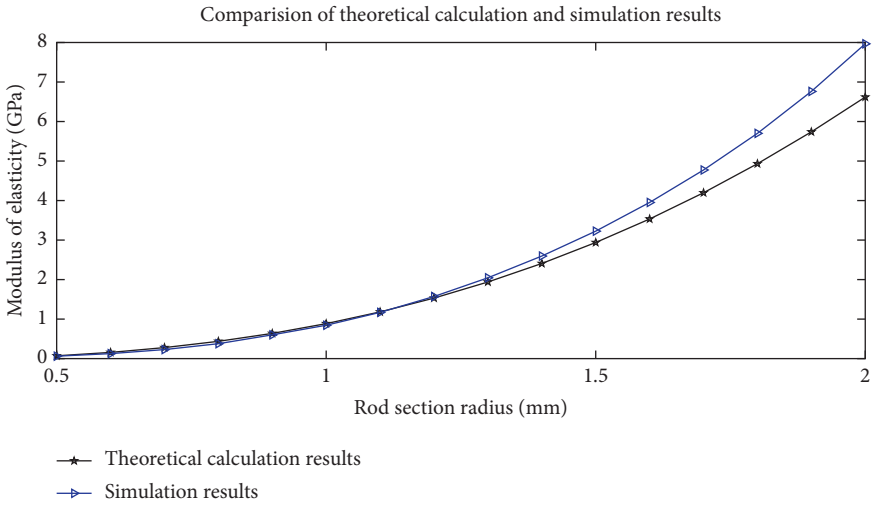

Figure 11: Comparison of theoretical and simulation results of equivalent modulus of elasticity.

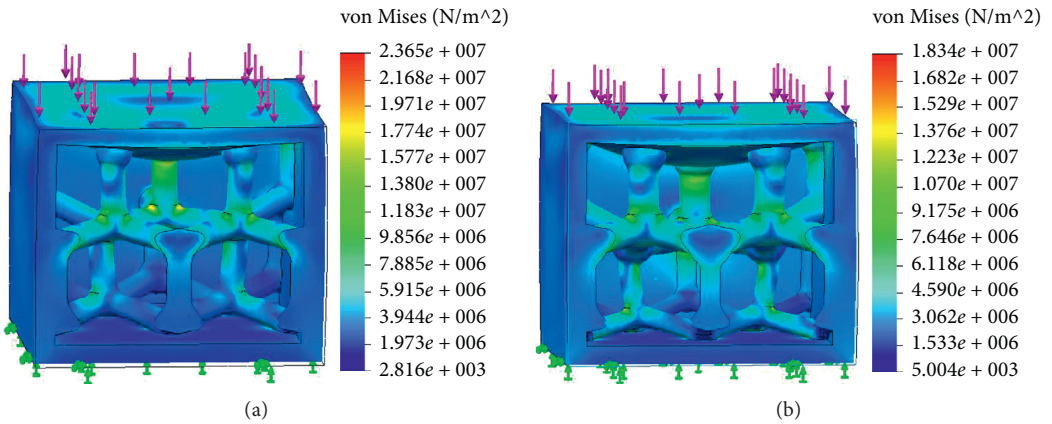

Figure 12: Comparison of stress state. (a) The superposition of constant density units ($r = 1$ mm). (b) The superposition of variable density units ($r = 1.2$ mm and 0.8 mm).

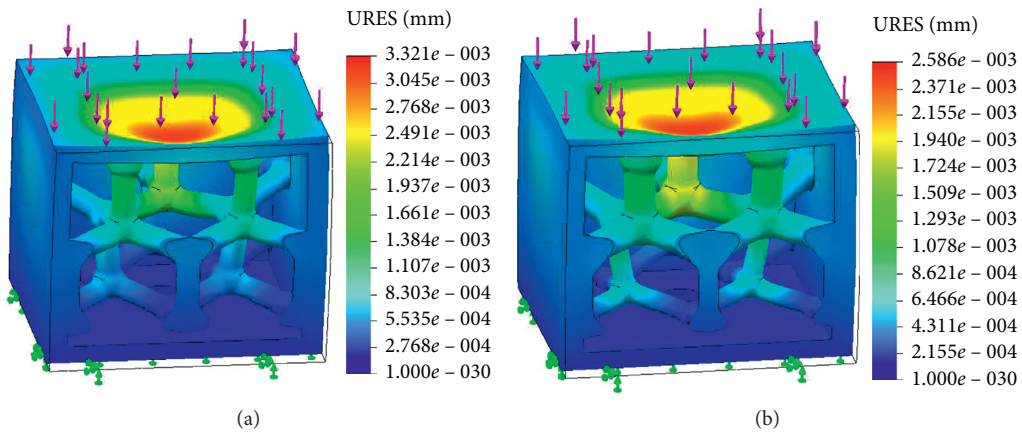

Figure 13: Comparison of displacement state. (a) The superposition of constant density units ($r = 1$ mm). (b) The superposition of variable density units ($r = 1.2$ mm and 0.8 mm).

Figure 14: Specimens with AM and their compression test.

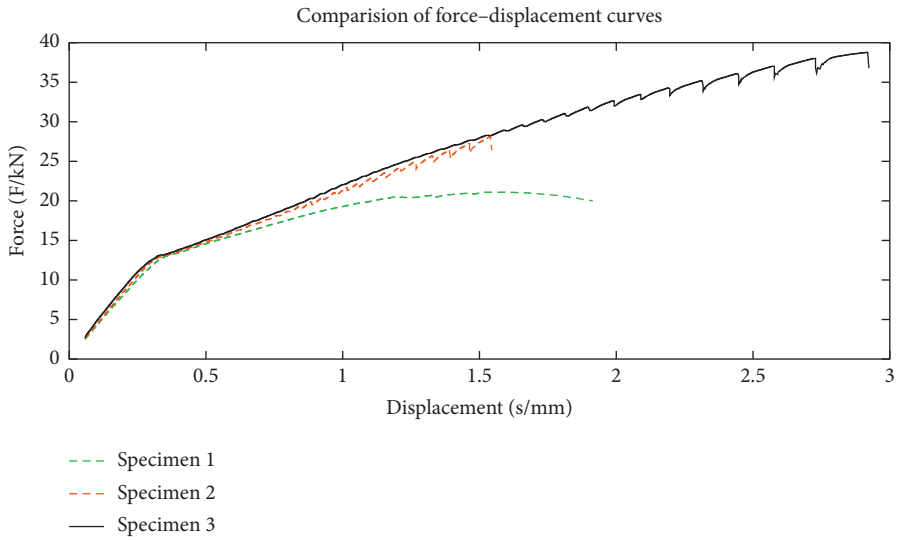

Figure 15: Comparison of force-displacement curves of three kinds of specimens.

Table 3: Analysis of test results of three kinds of specimens.

Name	Specimen 1	Specimen 2	Specimen 3
Quality (g)	31	31	31
Overall size (mm)	∅30 h40.66	∅30 h40.66	∅30 h40.66
Relative density	0.269	0.269	0.269
Yield displacement (mm)	0.3365	0.3290	0.3330
Yield load (kN)	13.04	12.91	13.13
Failure load (kN)	21.1	28.1	38.8
Failure time (s)	356.634	478.112	684.657
Equivalent modulus of elasticity by formula (GPa)	—	4.084	4.084
Equivalent modulus of elasticity by test (GPa)	4.103	4.155	4.175

obtained from the test results is 4.165, and the equivalent modulus of elasticity calculated from equation (19) is 4.084, the two are relatively consistent, which preliminarily proves the correctness of the theoretical research.

According to the comparison results of Figure 15 and Table 3, the following test conclusions can be obtained:

(i) Compared with the octahedral lattice structure; the diamond lattice structure shows better compressive properties in the strengthening stage.

(ii) The compressive strength of the variable density lattice structure adapted to local stress is higher than that of the uniform one.

(iii) The formula of equivalent modulus of elasticity studied in Section 2 has certain applicability.

5. Conclusion

The aim of this paper is to study the theoretical effect of relative density on the mechanical properties of the diamond lattice structure and to use this study to design a varying density lattice structure optimized for equivalent elastic modulus in compression based on additive manufacturing.

A highly detailed geometric model is developed to determine the exact volume of the diamond lattice within a greater cell superposition, thereby allowing an accurate determination of the relative density of the lattice structure given the rod diameter and diameter of inscribed circle representing the size of the unit fill space. The mathematical model of the relative density and mechanical properties of the unit is established, and the relationship between them is obtained. A series of simulations are carried out to verify them, and the results are relatively consistent. The data of compression test in Section 4 also confirms the correctness of the mathematical model accuracy.

The hypothesis of variable density is put forward and verified by simulation and experiment. The results show that the diamond lattice structure has more advantages than the traditional octahedral structure in compression, and the variable density diamond lattice structure whose density of the filling unit gradually decreasing with the stress point as the center has better compression performance.

Data Availability

The data used to support the findings of this study are available from the corresponding author upon request.

Conflicts of Interest

The authors declare that they have no conflicts of interest regarding the publication of this paper.

Acknowledgments

The authors received financial support provided by the National Natural Science Foundation of China (52075356), Excellent Innovation Project for Postgraduates in Shanxi Province (2018BY104), and the Natural Science Foundation of Shanxi Province (201801D221219, 201901D111236, and 201901D111246).

References

[1] C. Chu, G. Graf, and D. W. Rosen, "Design for additive manufacturing of cellular structure," *Computer-Aided Design and Applications*, vol. 5, no. 5, pp. 686–696, 2008.

[2] D. W. Rosen, "Research supporting principles for design for Additive Manufacturing," *Virtual and Physical Prototyping*, vol. 9, no. 4, pp. 225–232, 2014.

[3] M. K. Thompson, G. Moroni, T. Vaneker et al., "Design for additive manufacturing: trends, opportunities, considerations, and constraints," *CIRP Annals*, vol. 65, no. 2, pp. 737–760, 2016.

[4] M. Helou and S. Kara, "Design, analysis and manufacturing of lattice structures: an overview," *International Journal of Computer Integrated Manufacturing*, vol. 31, no. 3, pp. 243–261, 2018.

[5] J. Nguyen, P. Sang-In, and D. Rosen, "Heuristic optimization method for cellular structure design of light weight components," *International Journal of Precision Engineering and Manufacturing*, vol. 14, no. 6, pp. 1071–1078, 2013.

[6] Li Yang, "Experimental-assisted design development for an octahedral cellular structure using additive manufacturing," *Rapid Prototyping Journal*, vol. 21, no. 2, pp. 168–176, 2015.

[7] Li Yang, O. Harrysson, D. Cormier, H. West, H. Gong, and B. Stucker, "Additive Manufacturing of metal cellular structures: design and fabrication," *The Minerals, Metals and Materials Society*, vol. 67, no. 3, pp. 608–615, 2015.

[8] S. Vongbunyong and S. Kara, "Development of software tool for cellular structure integration for additive manufacturing," *Procedia CIRP*, vol. 48, pp. 489–494, 2016.

[9] H. Araujo, M. Leite, A. R. Ribeiro, A. M. Deus, L. Reis, and M. Fátima Vaz, "The effect of geometry on the flexural properties of cellular core, structures," *Proceedings of the Institution of Mechanical Engineers, Part L: Journal of Materials: Design and Applications*, vol. 3, pp. 338–347, 2019.

[10] J. G. Monteiro, M. Sardinha, and F. Alves, "Evaluation of the effect of core lattice topology on the properties of sandwich panels produced by additive manufacturing," *Proceedings of the Institution of Mechanical Engineers, Part L: Journal of Materials: Design and Applications*, pp. 1–13, 2020.

[11] Y. H. Ahmed, *The Development of Lightweight Cellular Structures for Metal Additive Manufacturing*, Dissertation. University of Exeter, Britain, UK, 2013.

[12] J. Kadkhodapour, H. Montazerian, A. C. Darabi et al., "Failure mechanisms of additively manufactured porous biomaterials: effects of porosity and type of unit cell," *Journal of the Mechanical Behavior of Biomedical Materials*, vol. 50, pp. 180–191, 2015.

[13] Y. Li, H. Jahr, P. Pavanram et al., "Additively manufactured functionally graded biodegradable porous iron," *Acta Biomaterialia*, vol. 96, pp. 646–661, 2019.

[14] B. N. Panda, *Design and Development of Cellular Structure for Additive Manufacturing*, Eng Dissertation. National Institute of Technology Rourkela, Rourkela, India, 2015.

[15] G.-H. Song, S.-K. Jing, F.-L. Zhao, Y.-D. Wang, H. Xing, and J.-T. Zhou, "Design optimization of irregular cellular structure for additive manufacturing," *Chinese Journal of Mechanical Engineering*, vol. 30, pp. 1184–1192, 2017.

[16] F.-L. Zhao, S.-K. Jing, and C.-Y. Liu, "Variable density cellular structure design method base on local relative density mapping," *Journal of Mechanical Engineering*, vol. 54, no. 19, pp. 121–128, 2018.

[17] J.-H. Liu, D.-P. Wang, and W.-T. Xu, "Design method of honeycomb structure generation for additive manufacturing," *Computer Integrated Manufacturing Systems*, vol. 23, no. 10, pp. 2101–2107, 2017.

[18] Z.-Y. Liao, Y.-J. Wang, and S.-T. Wang, "Graded-density lattice structure optimization design based on topology optimization," *Journal of Mechanical Engineering*, vol. 55, no. 8, pp. 65–72, 2019.

[19] H.-W. Liu, *Mechanics of Materials*, Higher Education Press, Beijing, China, 2004.

[20] Y.-X. Yu, "Reduced moment of inertia of variable cross-section members," *Hoisting and Conveying Machinery*, vol. 2, pp. 75–78, 1980.

[21] J. Gibson and M. F. Ashby, *Cellular Solids:Structure and Properties*, Cambridge University Press, Cambridge, UK, 1997.